Notes

Extra- and Intranuclear Dynamics and Distribution of Modified-PAMAM Polyplexes in Living Cells: A Single-Molecule Analysis

Seungah Lee, Kihoon Nam,[†] Jong-Sang Park,[†] Joon Sig Choi,[‡] Seong Kug Eo,[§] Dong Jin Yoo,[#] and Seong Ho Kang[*]

Department of Chemistry and Research Institute of Physics and Chemistry (RINPAC), Chonbuk National University, Jeonju 561-756, Korea. [*]E-mail: shkang@chonbuk.ac.kr
[†]School of Chemistry and Molecular Engineering, Seoul National University, Seoul 151-742, Korea
[‡]Department of Biochemistry, Chungnam National University, Daejeon 305-764, Korea
[§]College of Veterinary Medicine and Bio-Safety Research Institute, Chonbuk National University, Jeonju 561-756, Korea
[#]Department of Chemistry, Seonam University, Namwon 590-711, Korea
Received March 6, 2008

Key Words : PAMAM dendrimer, Extra- and intranuclear dynamics, Polyplexes, Single-molecule analysis

Recently, research into gene therapy has expanded to the identification of a suitable gene delivery vector that can achieve high transgenic gene expression efficiency without toxicity. Over the past decade, various types of cationic lipids,[1,2] polypeptides,[3-5] surfactants[6,7] and liposomes[8-12] have been introduced as prospective alternatives to enhance the gene delivery efficiency of plasmid DNA and oligonucleotides. In particular, polyamidoamine (PAMAM) dendrimers, which are polycationic synthetic polymers, can be used for gene transfer because they form stable polyplexes with plasmid DNA or oligonucleotides and exhibit moderate cytotoxicity and substantial gene delivery activity.[13-20] A previous report described the development of surface-modified PAMAM derivatives with arginine (R) or lysine (K) called PAMAM-R and PAMAM-K, respectively.[21] However, the dynamics and behavior of these modified PAMAM/DNA polyplexes in the cell interior are not completely understood on the single-molecule level.

Total internal reflection fluorescence microscopy (TIRFM) has been applied successfully in a variety of fields, such as real-time detection at solid/liquid interfaces,[22] cellular adhesion processes,[23] polymer-surface interactions,[24] protein-substrate adsorption[25] and signal transduction studies,[26] on account of its low fluctuations in background noise. However, the use of a single fluorescence detection system makes it difficult to obtain individual imaging and dynamics information from two or more different molecules within the living cells, simultaneously.

Therefore, a new approach is required to provide much more detailed information than that obtained using conventional methods. In order to solve this problem, an optics-based combined system that accommodates a multimode microscope of dual-color TIRFM and four-dimensional differential interference contrast (4D DIC) was constructed. Here, DIC imaging of the cell was used to provide information on the location of the intracellular polyplexes as well as the precise shape of a living HeLa cell as a function of time. In particular, 4D DIC imaging was used to examine the detailed living cell structure and three-dimensional (3D) positions of the nuclei and polyplexes in a cell, which were identified from a set of images recorded in multiple focal planes. In this study, an attempt was made to detect two different types of polyplexes (*i.e.* PAMAM-R-Alexa 633/DNA and PAMAM-K-Alexa 488/DNA) simultaneously in the same view field of a cover glass using a home-made combined optic system (Figure 1) in order to confirm the pathway of each polyplex in the extra- and intranuclear sites of a living HeLa cell.

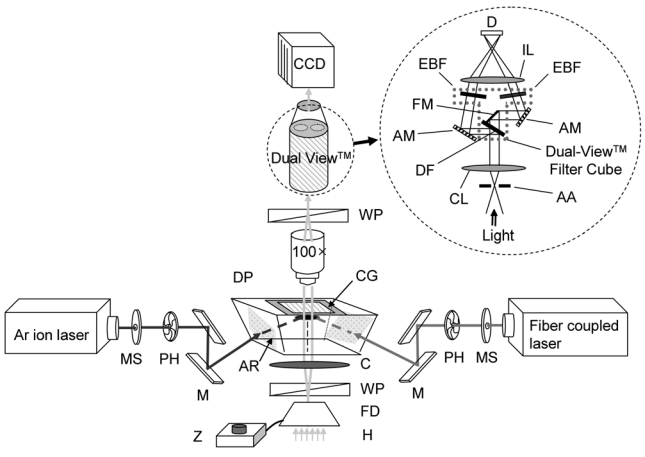

Figure 1. Schematic diagram of the home-made combined dual-color TIRFM and 4D Nomarski DIC system used for direct monitoring of the efficient transfer of polyplexes in living cells using a single microscope. Indicates: MS, mechanical shutter; PH, pinhole; M, mirror; H, halogen lamp; FD, field diaphragm; WP, wollaston prism; C, condenser; CG, cover glass; DP, all-side polished dove prism; AR, anti reflection; Z, z-motor; D, detector; IL, imaging lens; EBF, emission/barrier filter; AM, adjustable mirror; AA, adjustable aperture; CL, collimating lens; DF, dichroic filter; FM, fixed mirror.

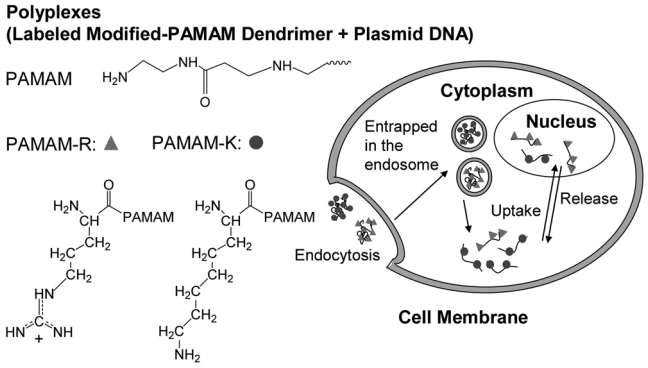

Figure 2. The mechanism for transferring the plasmid DNA into living HeLa cells using the modified PAMAM polyplexes containing the plasmid DNA.[30] *Indicate: triangle = PAMAM-R and circular = PAMAM-K.

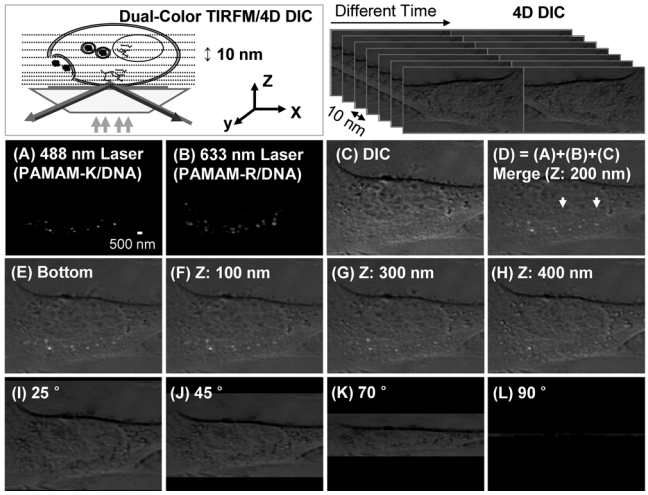

Figure 3. The location of the polyplexes using the combined dual-color TIRFM and 4D Nomarski DIC system. Representative images: (A) TIRFM image of PAMAM-K-Alexa488/DNA, (B) TIRFM image of PAMAM-R-Alexa633/DNA, (C) DIC image, (D) merged images of A, B and C. (E) through (H) are TIRFM and DIC merged images at different focal planes. (I) through (L) are 4D TIRFM images of the reconstructed sequential 3D TIRFM images of the two-polyplexes associated with the living HeLa cells at a different angle. A, B, C and D: dual-color TIRFM and DIC images of the polyplex located at 200 nm from the bottom of the cell. Optical slices from the bottom to the top of the cell at 10 nm intervals.

In modified-two polyplexes with the protonated surface, the polyplexes first attach to the cell membrane and are taken up into the cytoplasm *via* membrane perturbations or endocytosis (Figure 2). After being entrapped in the endosome, the two modified polyplexes with different properties migrate individually into the interior/exterior of the nucleus. Single-color TIRFM does not allow the different properties of the polyplexes in a cell to be detected simultaneously. In this case, the calculation was unable to represent accurately the differences between the two polyplexes in the intracellular localizations and dynamics. Therefore, an attempt was made to detect the two different polyplexes simultaneously using the combined system of dual-color TIRFM and 4D DIC (Figure 3). The 4D DIC microscope is an automated system equipped with a z-motor that records the DIC microscopic images in multiple focal planes and at multiple time-points and angles. 4D TIRFM/DIC images were obtained by the slicing cell at 10 nm intervals using the z-motor at multiple time-points, and the 3-dimensional image that can be rotated to show details of the cell was reconstructed using MetaMorph software. Figures 3A-3D show the polyplexes detected in the evanescent field layer, which is approximately 200 nm into the cell from the bottom of the cell, using dual-color TIRFM and 4D DIC. Each of the two different polyplexes was conjugated with Alexa Fluor®488 (green colors in Figure 3A) and Alexa Fluor®633 (red colors in Figure 3B) dyes to allow the two different lasers to be used simultaneously. The outline of a living HeLa cell could be observed on the DIC image (Figure 3C). Figure 3D shows the image merged with the dual-color TIRFM and DIC image. The results showed that the PAMAM-R-Alexa633/DNA polyplexes enter the nucleus from the cytoplasm more than the PAMAM-K-Alexa488/DNA polyplexes in the same single living cell at 4 h. The colocalization of the two modified polyplexes in a living HeLa cell was confirmed by 4D analysis of both dual-color TIRFM and DIC images by serially slicing at 10 nm vertical intervals. Figures 3E-3H show the dual-color TIRFM and 4D DIC combined images of the two-polyplexes at the upper part of multi-focal plane in the evanescent field layer. Sequential 3D images were

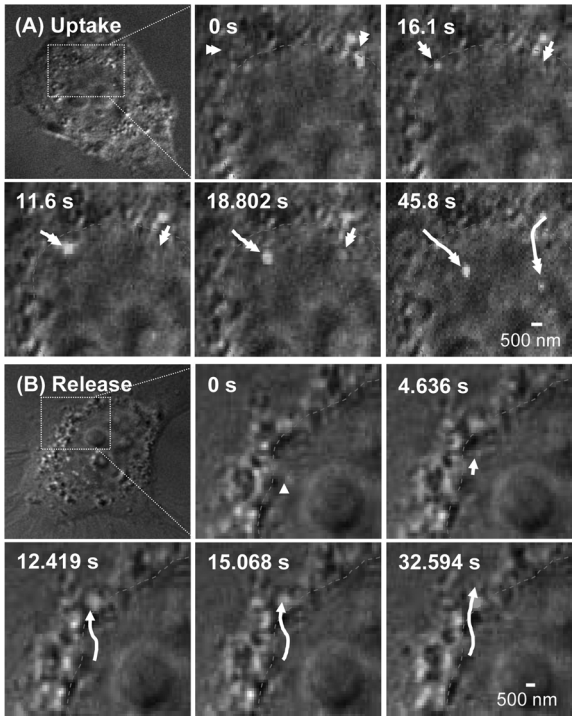

Figure 4. The real-time uptake (A) and release (B) of the polyplexes into a living HeLa cell using the combined dual-color TIRFM and 4D Nomarski DIC system. Polymer, PAMAM-K-Alexa488/DNA polyplexes; detection time, 2 h 30 min (uptake, two head arrow) and 3 h (release, one head arrow). The tails of the arrow show the moving-trace of each polyplex. The red dotted line indicates the nuclear membrane. The other conditions were the same as those shown in Figure 3.

collected and processed to construct a 4D projection in multiple focal planes. The reconstructed 4D images could be viewed from a number of angles (Figures 3I-3L). The images showed that the polyplexes located approximately 200 nm (white arrows in Figure 3D) from the bottom of the cell and the PAMAM-R-Alexa633/DNA polyplexes (red color) were more efficient in transfection towards the nucleus than the PAMAM-K-Alexa488/DNA polyplexes (green color) in the same single living cell at 4 h. On the other hand, the lower part or upper part of the same living cell did not show any polyplexes towards the nucleus.

There was a more irregular increased or decreased in the number of PAMAM-K polyplexes toward the nucleus with time than PAMAM-R polyplexes. Figure 4 shows the time-lapse images of the uptake (Figure 4A) and release (Figure 4B) of the PAMAM-K-Alexa488 polyplexes at 2 h 30 min (uptake) and 3 h (release) after incubating the polyplexes and the cell. In addition, a real-time moving-trace of each polyplex in a living cell could be produced at the single-molecule level. Overall, this method for monitoring the polyplexes inside a living cell using the combined optic system is expected to be a powerful technique in nano-bio technology.

Experimental Section

Fluorescent-dye Labeled PAMAM-R and PAMAM-K. PAMAM-R and PAMAM-K were synthesized according to the methodology reported elsewhere.[21] The labeling procedure of the modified-PAMAM is as follows: Alexa Fluor® dye (Molecular Probes, USA) was freshly dissolved in DMSO (2 mg/mL) and added drop-wise to a PAMAM dendrimer solution in a 0.2 M sodium carbonate buffer (pH 8.3). The PAMAM to Alexa Fluor® dye molar ratio was 1:1. The reaction was allowed to proceed in the dark for 2 h at 4 °C. The unbound Alexa Fluor® dye was removed using a pre-packed size exclusion column, NAPTM 25 (Sephadex G-25 DNA grade, Amersham Biosciences, USA), and the buffer was removed by overnight dialysis at 4 °C. The PAMAM-Alexa Fluor® dye fractions were combined as polyplexes and freeze-dried.

Plasmid Preparation. The luciferase expression plasmid (pCN-Luci) was constructed by subcloning the cDNA of *Photinus pyralis* luciferase with a 21-amino acid nuclear localization signal from the SV40 large T antigen to pCN.[27] The plasmid DNA was transformed into *E. coli* TOP10 competent cells. The highly-purified covalently-closed-circular-plasmid DNA was then purified using a QiaFilter purchased from Qiagen (Valencia, CA, USA) according to the manufacturer's instructions. The plasmid was precipitated in isopropanol, washed twice with 70% ethanol and re-suspended in distilled water.

Preparation of the Modified-PAMAM with Plasmid DNA. The fluorescent labeled-dendrimers (Alexa Fluor®633-labeled PAMAM-R and Alexa Fluor®488-labeled PAMAM-K) and 0.5 μg of the plasmid DNA were mixed to form polyplexes at a charge ratio of 6 in 600 μL of serum-free DMEM. This charge ratio was found to be sufficient for the formation of complete complexes, and PAMAM-R and PAMAM-K could form complexes that exposed multiple surplus surfaces of the R and K residues.[21] The mixture was incubated for 30 min at room temperature. The polyplexes were then added to the cells and incubated. Sampling was carried out at different time points.

Cell Culture. The HeLa cells (ATCC, Rockville, MD, USA) were grown in DMEM (pH 7.2, Dulbecco's modified eagles medium, GIBCO, Gaithersburg, MD, USA) containing 10% FBS (Fetal bovine serum, GIBCO) and 1× antibiotic-antimycotic agent. The cells were maintained on plastic tissue culture dishes (Falcon) at 37 °C in an incubator with a humidified atmosphere containing 5% CO_2/95% air. The HeLa cells were plated (22 mm sq., No. 1 Dow Corning, Corning, NY, USA) on a culture dish (35 × 10 mm, Suwon Plastic Labware, Korea) at a density of ~2×10^4 cells per bare cover glass, and a medium containing serum was changed to serum-free medium prior to transfection. The adherent cells were rinsed twice with DPBS to remove the polyplexes that were not bound to the cells immediately before detection. The cover glass was placed on an all-side polished dove prism (BK7, 15 mm × 63 mm × 15 mm, n = 1.522, Korea Electro-Optics Co., LTD., Korea).

Home-made Combined System of Dual-color TIRFM and 4D DIC. An upright Olympus BX51 microscope (Olympus Optical Co., LTD, Tokyo, Japan) equipped with a Dual-View™ (Optical Insight, LLC, Tucson), a DIC slider (U-DICT, Olympus) and a Z-motor was used for most observations (Figure 1). A TIRFM with a nanometer precision positioning controller (Digital Bio Technology Co., LTD, Seoul, Korea) was constructed. An Olympus UPLFL 100× oil immersion objective with a numerical aperture of 1.3 and a working distance of 0.1 mm was used. A CCD camera (Cascade 512B, Photometrics, Tucson, AZ, USA) was mounted on top of the microscope with a halogen lamp as the illumination source. An argon ion laser at 488 nm (model 532-LAP-431-220, Melles Griot, Irvin, CA, USA) and a fiber-coupled laser at 635 nm (B&W TEK Inc., Newark, DE, USA) were used as the excitation sources for the dual-color TIRFM work. The Dual-View™ was mounted between the objective lens and CCD camera.[28,29] The emission signals were separated using two types of optical splitters. The CCD exposure time was 100 ms and the gain was 3030. The cover glass (No.1 Corning, 22 mm square) used to incubate the cells was placed on the all-side polished dove prism (BK7, 15 mm × 63 mm × 15 mm, n = 1.522, Korea Electro-Optics Co., LTD., Korea) for the combined the 4D Nomarksi DIC and dual-color TIRF on a single camera. The cover glass and prism were index-matched with a drop of immersion oil (Immersol™ 518F, Zeiss, n = 1.518). The laser beam was directed through the prism toward the cover glass/media interface. The incidence angle θ_i was slightly higher than 72°. Two Uniblitz mechanical shutters were used to block the laser beam when the camera was turned off.[28,29] Image collection and raw stacks were split into a single image using MetaMorph® 6.3 software (Universal Imaging Co., Downing town, PA, USA).

Acknowledgments. This work was supported by a grant from Korea Science & Engineering Foundation (R01-2007-000-20238-0).

References

1. Alahari, S. K.; DeLong, R.; Fisher, M. H.; Dean, N. M.; Viliet, P.; Juliano, R. L. *J. Pharmacol. Exp. Ther.* **1998**, *286*, 419.
2. Bennett, C. F.; Chiang, M. Y.; Chan, H.; Shoemaker, J. E.; Mirabelli, C. K. *Mol. Pharmacol.* **1992**, *41*, 1023.
3. Chaloin, L.; Vidal, P.; Lory, P.; Mery, J.; Lautredou, N.; Divita, G.; Heitz, F. *Biochem. Biophy. Res. Commun.* **1998**, *243*, 601.
4. Rajur, S. B.; Roth, C. M.; Morgan, J. R.; Yarmush, M. L. *Bioconjug. Chem.* **1997**, *8*, 935.
5. Degols, G.; Leonetti, J. P.; Lebleu, B. *Ann. NY Acad. Sci.* **1992**, *660*, 331.
6. Hughes, J. A.; Aronsohn, A. I.; Avrutskaya, A. V.; Juliano, R. L. *Pharm. Res.* **1996**, *13*, 404.
7. Liang, E.; Hughes, J. *Biochim. Biophys. Acta* **1998**, *1369*, 39.
8. Gao, X.; Huang, L. *Gene Ther.* **1995**, *2*, 710.
9. De Oliveira, M. C.; Fattal, E.; Couvreur, P.; Lesieur, P.; Bourgaux, C.; Ollivon, M.; Dubernet, C. *Biochim. Biophys. Acta* **1998**, *1372*, 301.
10. Tari, A.; Khodadadian, M.; Ellerson, D.; Deisseroth, A.; Lopez-Berestein, G. *Leuk. Lymphoma.* **1996**, *21*, 93.
11. Felgner, P. L.; Tsai, Y. J.; Sukhu, L.; Wheeler, C. J.; Manthorpe, M.; Marshall, J.; Cheng, S. H. *Ann. NY Acad. Sci.* **1995**, *772*, 126.
12. Zabner, J.; Fasbender, A. J.; Moninger, T.; Poellinger, K. A.; Welsh, M. J. *J. Biol. Chem.* **1995**, *270*, 18997.
13. Yoo, H.; Sazani, P.; Juliano, R. L. *Pharm. Res.* **1999**, *16*, 1799.
14. Hughes, J. A.; Aronsohn, A. I.; Avrutskaya, A. V.; Juliano, R. L. *Pharm. Res.* **1996**, *13*, 404.
15. Bielinska, A.; Kukowska-Latallo, J. F.; Johnson, J.; Tomalia, D. A.; Baker, J. R. Jr. *Nucleic Acids Res.* **1996**, *24*, 2176.
16. Delong, R.; Stephenson, K.; Loftus, T.; Fisher, M.; Alahari, S.; Nolting, A.; Juliano, R. L. *J. Pharm. Sci.* **1997**, *86*, 762.
17. Haensler, J.; Szoka, F. C. Jr. *Bioconjug. Chem.* **1993**, *4*, 372.
18. Kukowska-Latallo, J. F.; Bielinska, A. U.; Johnson, J.; Spindler, R.; Tomalia, D. A.; Baker, J. R. Jr. *PNAS* **1996**, *93*, 4897.
19. Qin, L.; Pahud, D. R.; Ding, Y.; Bielinska, A. U.; Kukowska-Latallo, J. F.; Baker, J. R. Jr.; Bromberg, J. S. *Hum. Gene Ther.* **1998**, *9*, 553.
20. Tang, M. X.; Redemann, C. T.; Szoka, F. C. Jr. *Bioconjug. Chem.* **1996**, *7*, 703.
21. Choi, J. S.; Nam, K.; Park, J. Y.; Kim, J. B.; Lee, J. K.; Park, J. S. *J. Control Release* **2004**, *99*, 445.
22. Jeong, S. J.; Park, S.-K.; Chang, J. K.; Kang, S. H. *Bull. Korean Chem. Soc.* **2005**, *26*, 979.
23. Yang, D. M.; Huang, C. C.; Lin, H. Y.; Tsai, D. P.; Kao, L. S.; Chi, C. W.; Lin, C. C. *J. Microsc.* **2003**, *209*, 223.
24. Rebar, V. A.; Santore, M. M. *Macromolecules* **1996**, *29*, 6262.
25. Roth, C. M.; Lenhoff, A. M. *Langmuir* **1995**, *11*, 3500.
26. Mashanov, G. I.; Tacon, D.; Peckham, M.; Molloy, J. E. *J. Biol. Chem.* **2004**, *279*, 15274.
27. Lee, M. J.; Cho, S. S.; You, J. R.; Lee, Y.; Kang, B. D.; Choi, J. S.; Park, J. W.; Suh, Y. L.; Kim, J. A.; Kim, D. K.; Park, J. S. *Gene Ther.* **2002**, *9*, 859.
28. Kang, S. H.; Kim, Y.-J.; Yeung, E. S. *Anal. Bioanal. Chem.* **2007**, *387*, 2663.
29. Kim, D.; Lee, H. G.; Jung, H.; Kang, S. H. *Bull. Korean Chem. Soc.* **2007**, *28*, 783.
30. Dvornic, P. R.; Tomalia, D. A. *Sci. Spectra* **1996**, *5*, 36.